Soil metabolomics and bacterial functional traits revealed the responses of rhizosphere soil bacterial community to long-term continuous cropping of Tibetan barley

Yuan Zhao [Equal first author, 1], **Youhua Yao** [Equal first author, 2], **Hongyan Xu** [1, 2], **Zhanling Xie** [Corresp., 1], **Jing Guo** [1], **Zhifan Qi** [1], **Hongchen Jiang** [3]

[1] Qinghai University, College of Eco-Environmental Engineering, Xining, Qinghai, China

[2] Qinghai University, Academy of Agriculture and Forestry Sciences, Xining, Qinghai, China

[3] China University of Geosciences, State Key Laboratory of Biogeology and Environmental Geology, Wuhan, Hubei, China

Corresponding Author: Zhanling Xie
Email address: xiezhanling2012@126.com

Continuous cropping often leads to an unbalanced soil microbial community, which in turn negatively affects soil functions. However, systematic research of how these effects impact the bacterial composition, microbial functional traits, and soil metabolites is lacking. In the present study, the rhizosphere soil samples of Tibetan barley continuously mono-cropped for 2 (CCY02), 5 (CCY05), and 10 (CCY10) years were collected. By utilizing 16S high-throughput sequencing, untargeted metabolomes, and quantitative microbial element cycling smart chips, we examined the bacterial community structure, soil metabolites, and bacterial functional gene abundances, respectively. We found that bacterial richness (based on Chao1 and Phylogenetic Diversity [PD] indices) was significantly higher in CCY02 and CCY10 than in CCY05. As per principal component analysis (PCA), samples from the same mono-cropped year tended to share more similar species compositions and soil metabolites, and exhibited distinct patterns over time. The results of the Procrustes analysis indicated that alterations in the soil metabolic profiles and bacterial functional genes after long-term continuous cropping were mainly mediated by soil microbial communities ($P < 0.05$). Moreover, 14 genera mainly contributed to the sample dissimilarities. Of these, five genera were identified as the dominant shared taxa, including *Blastococcus*, *Nocardioides*, *Sphingomonas*, *Bacillus*, and *Solirubrobacter*. The continuous cropping of Tibetan barley significantly increased the abundances of genes related to C-degradation ($F = 9.25$, $P = 0.01$) and P-cycling ($F = 5.35$, $P = 0.03$). N-cycling significantly negatively correlated with bacterial diversity ($r = -0.71$, $P = 0.01$). The co-occurrence network analysis revealed that nine hub genera correlated with most of the functional genes and a hub taxon, Desulfuromonadales, mainly co-occurred with the metabolites via both negative and positive correlations. Collectively, our findings indicated that continuous

cropping significantly altered the bacterial community structure, functioning of rhizosphere soils, and soil metabolites, thereby providing a comprehensive understanding of the effects of the long-term continuous cropping of Tibetan barley.

Soil Metabolomics and Bacterial Functional Traits Revealed the Responses of Rhizosphere Soil Bacterial Community to Long-term Continuous Cropping of Tibetan Barley

Yuan Zhao[#1], YouhuaYao[#2], Hongyan Xu[1,2], Zhanling Xie*[1], Jing Guo[1], Zhifan Qi[1], Hongchen Jiang[3]

[1]College of Eco-Environmental Engineering, Qinghai University, Xining, Qinghai, China
[2]Academy of Agriculture and Forestry Sciences, Qinghai University, Xining, Qinghai, China
[3]State Key Laboratory of Biogeology and Environmental Geology, China University of Geosciences, Wuhan, China

Corresponding Author:
Zhanling Xie [1]
Ningda Road 251, Xining, Qinghai, 810016, China
Email address: xiezhanling2012@126.com

Abstract

Continuous cropping often leads to an unbalanced soil microbial community, which in turn negatively affects soil functions. However, systematic research of how these effects impact the bacterial composition, microbial functional traits, and soil metabolites is lacking. In the present study, the rhizosphere soil samples of Tibetan barley continuously mono-cropped for 2 (CCY02), 5 (CCY05), and 10 (CCY10) years were collected. By utilizing 16S high-throughput sequencing, untargeted metabolomes, and quantitative microbial element cycling smart chips, we examined the bacterial community structure, soil metabolites, and bacterial functional gene abundances, respectively. We found that bacterial richness (based on Chao1 and Phylogenetic Diversity [PD] indices) was significantly higher in CCY02 and CCY10 than in CCY05. As per principal component analysis (PCA), samples from the same mono-cropped year tended to share more similar species compositions and soil metabolites, and exhibited distinct patterns over time. The results of the Procrustes analysis indicated that alterations in the soil metabolic profiles and bacterial functional genes after long-term continuous cropping were mainly mediated by soil microbial communities ($P < 0.05$). Moreover, 14 genera mainly contributed to the sample dissimilarities. Of these, five genera were identified as the dominant shared taxa, including *Blastococcus*, *Nocardioides*, *Sphingomonas*, *Bacillus*, and *Solirubrobacter*. The continuous cropping of Tibetan barley significantly increased the abundances of genes related to C-

degradation ($F = 9.25$, $P = 0.01$) and P-cycling ($F = 5.35$, $P = 0.03$). N-cycling significantly negatively correlated with bacterial diversity ($r = -0.71$, $P = 0.01$). The co-occurrence network analysis revealed that nine hub genera correlated with most of the functional genes and a hub taxon, Desulfuromonadales, mainly co-occurred with the metabolites via both negative and positive correlations. Collectively, our findings indicated that continuous cropping significantly altered the bacterial community structure, functioning of rhizosphere soils, and soil metabolites, thereby providing a comprehensive understanding of the effects of the long-term continuous cropping of Tibetan barley.

Keywords: Tibetan barley; continuous cropping; rhizosphere bacterial community; metabolomic; elemental cycling genes.

Introduction

Soil health sustains the capacity of agricultural soils for ecosystem functioning and thrives as a living ecosystem for microbes, plants, and insects (Lal 2016; Rinot et al. 2019). However, continuous cropping, especially of a monoculture consisting of one plant type in the same agricultural field with standard and persistent agronomic practices, usually leads to crop yield reductions, soil aggregation, soil physicochemical property alterations, and soil microbial community changes, ultimately exerting negative effects on soil health (Murphy & Lemerle 2006; Pervaiz et al. 2020). Soil microbiota play crucial roles in the maintenance of soil functions and significantly affect agricultural soil productivity, plant growth, and crop quality (Bello-Akinosho et al. 2016; Huang et al. 2013; Pii et al. 2016). Previous studies demonstrated that continuous monoculture greatly affected the structure of the rhizosphere soil microbial community. For example, successive monoculture practices were found to decrease bacterial community diversity (Sun et al. 2018), increase harmful populations, and inhibit beneficial ones (Gao et al. 2019). In our previous study, we found that the continuous cropping of Tibetan barley resulted in a significant decline in crop yields and bacterial community diversity, as well as increased the relative abundances of bacteria associated with chemo-heterotrophy, aromatic compound degradation, and nitrate reduction, per a FaProTax prediction (Yao et al. 2020). However, research on how continuous cropping practices affect soil microbial functional traits is lacking.

Nutrient cycling, including carbon (C), nitrogen (N), and phosphorus (P), is a common problem that has been investigated on a global scale (Zhang et al. 2019). The tight interactions in the rhizosphere zone between plants and soil microbiota affect the stability of nutrient cycling in the soil (Zhang et al. 2019). For example, Kuzyakov et al. (2010) reported that soil microbial activity was enhanced by a substantial source of soil C from root secretion and deposition. Yu et al. (2019) found that the activities of key functional genes within the microbial community involved in N-cycling increased along with a reduction in N application during maize/soybean strip

intercropping. Alami et al. (2020) found that the abundances of soil N functional genes significantly differed between cultivated and fallow fields across two seasons based on a PICRUSt prediction. Pang et al. (2021) indicated that the continuous cropping of sugarcane significantly decreased the bacterial abundances associated with rhizosphere soil N- and sulfur (S)-cycling, thereby decreasing the abundances of N translocation genes and dissimilatory reduction genes, as determined by the soil metagenome. Unfortunately, less is known about soil functional gene cycling and their interactions with microbial communities underlying the continuous cropping of Tibetan barley.

Most studies on continuous cropping have generally focused on changes in the microbial community and their interactions with soil properties, while soil metabolite composition is rarely discussed. The rhizosphere, which is a hub of microbial activities, increases the nutrient supply for microorganisms, as the roots release several organic compounds that influence plant growth and health (Pinton et al. 2007). Thus, soil metabolomics can potentially enhance our understanding of this chemical exchange. Fortunately, the development of untargeted metabolomics has allowed us to detect and identify increasingly more compounds that are secreted by plants and the organisms that interact with them in the rhizosphere (Swenson et al. 2015; Withers et al. 2020). For example, Wang et al. (2020) studied the continuous cropping of ramie by combining rhizosphere microbe identification and non-targeted gas chromatograph-mass spectrometer (GS/MS) metabolome analysis, and found that bacteria, such as Rhizobia, synthesized IAA and likely reduced the biotic stress of ramie. Nevertheless, the contribution of the changes in soil metabolites, their co-occurrence network, and microbial composition on the long-term monoculture of crops are far less understood, especially in Tibetan barley.

Thus, in this study, we collected the rhizosphere soils of Tibetan barley after two short-term and one long-term periods of cropping. By applying high-throughput sequencing and liquid chromatography mass spectrometry (LC-MS) untargeted metabolomics, we investigated the change trends in soil bacterial community structures and differences in soil metabolites. By constructing a co-occurrence network, we determined the changes in the interactions of bacterial communities. Quantitative microbial element cycling (QMEC) was applied to detect the abundances of C-, N-, P-, and S-cycling-related genes in the rhizosphere soils of different continuous cropping years (Zheng et al. 2018). Our findings will enhance our understanding of the effects of the long-term continuous cropping of Tibetan barley on the direct interactions between specific functional taxa and important functional gene metabolism, and provide a comprehensive understanding of the effects of the long-term continuous cropping of Tibetan barley.

Materials & Methods

Site description and rhizosphere soil sampling

The study was carried out at an alpine Tibetan barley experiment site located in the Qinghai–Tibetan Plateau (37°21′N, 101°43′E; altitude, 3700 m), Beishan township, Menyuan county, Qinghai Province, China. This region has a plateau continental climate with a mean annual temperature of 1.3°C and mean annual precipitation of 530–560 mm. According to the Food and Agriculture Organization (FAO) classification, the soil type is classified as Kastanozems (Schad & Spaargaren 2006). Kunlun 14 barley (Hordeum vulgare L.) was used as the experiment material. The study site consisted of independent plots over many years of the successive monoculture of Tibetan barley. Tibetan barley seeds were cultivated in April each year after the annual application of blended fertilizer and harvested in August following previously described methods (Yao et al. 2020). Briefly, in July 2020, we selected three study plots, including 2, 5, and 10 years of successive monocropping of Tibetan barley, which we named CCY02, CCY05, and CCY10, respectively. Each plot contained five sites, and 15 rhizosphere soil samples (closely adhered to the roots) were collected in a "Z" pattern and mixed as an individual sample with four replicates. Soil samples were immediately transferred on ice to the laboratory and stored at −20°C for subsequent analysis.

High-throughput sequencing of bacterial 16S rRNA gene

Total genomic DNA from each rhizosphere soil sample was extracted using an E.Z.N.A. ® Soil DNA kit (Omega Bio-Tek, Norcross, GA, USA) following the manufacturer's instructions. DNA was amplified with the primer set, 338F (5'-ACT CCT ACG GGA GGC AGC AG-3') and 806R (5'-GGA CTA CHV GGG TWT CTA AT-3'), targeting the V3–V4 hypervariable region of the bacterial 16S rRNA gene (Zeng & An 2021). PCR amplification and purification were performed following previously described methods (Yang et al. 2019). Finally, the DNA products were sequenced on an Illumina MiSeq platform (Majorbio, Shanghai, China).

Soil non-targeted metabolomic detection and analysis

Twelve rhizosphere soil samples were sent to Majorbio (Shanghai, China) on dry ice for metabolite extraction, detection, and analysis. In detail, 1,000-mg soil aliquot of each sample was homogenized with 1,000 μL methanol/water (4:1, v/v) solution, including 0.02 mg/mL internal standard (L-2-chlorophenylamine acid) for 6 min at −10°C and 50 kHz using a Geno-grinder 2,000 (SPEX, Metuchen, NJ, USA) and spun down for 30 min at 5°C and 40 kHz. After placing for 30 min at −20°C, each material was centrifuged at 13,000 g (relative centrifugal force) for 15 min at 4°C, then the supernatant was transferred and concentrated by a Termovap Sample Concentrator (DC-24, Anpel Laboratory Technologies, Shanghai, China). The dry residue was derivatized by adding 50 μL acetonitrile/water (1:1), homogenized for 30 s at 5°C and 40 kHz, and centrifuged at 13,000 g (relative centrifugal force) for 10 min at 4°C. Finally, the supernatant

was subjected to LC-tandem MS (MS/MS) analysis; 20 μL supernatant of each sample was mixed for the quality control sample.

Chromatographic separation of the metabolites was performed using a UHPLC-Triple TOF system (AB Sciex, Foster City, CA, USA) equipped with an ACQUITY UPLC HSS T3 (100 mm × 2.1 mm i.d., 1.8 μm; Waters, Milford, CT, USA). Mobile phase A contained 95% water and 5% acetonitrile (with 0.1% formic acid), while mobile phase B contained 5% water (with 0.1% formic acid), 47.5% acetonitrile, and 47.5% isopropanol. The UPLC system was coupled to a quadrupole time-of-flight mass spectrometer (Triple TOFTM 5600þ; AB Sciex, Foster City, CA, USA) equipped with an electrospray ionization source operating in positive and negative modes. Data were analyzed using an online analysis platform (Majorbio, Shanghai, China) following the online instructions. Briefly, the image data were imported into the metabolomics processing software ProgenesisQI (Waters Corp., Milford, CT, USA) for baseline filtering, peak recognition, integration, retention time correction, and peak alignment, which produced the retention time, mass charge ratio, peak intensity, and data matrix. Then, the characteristic peak was detected and the information from the MS and MS/MS analyses was mapped with a metabolic specific database; the mass error was set to < 10 PPM. Finally, the metabolites were identified according to the matching scores of the secondary MS. The data were normalized with Pareto scaling and log-transformed before further analysis.

QMEC

Twelve qualified soil DNA samples were sent to Guangdong Magigene Biotechnology Co., Ltd. (Guangzhou, China) for QMEC analysis, wherein a high-throughput quantitative PCR (qPCR)-based chip was applied to assess the microbial functional potential, including 71 functional genes related to C-, N-, P-, and S-cycling (Zheng et al. 2018). QMEC manipulation was conducted following previously described methods (Chen et al. 2020a). Briefly, DNA templates and qPCR reagents were added to the sample source-plate; each primer and qPCR reagent was added to a separate source-plate. In each run, 100-nL reactions were first mixed using an automated high-throughput sample preparation device, then added to the nanopore of the qPCR chip on a Wafergen Smart-Chip Real-time PCR platform (Wafergen, Fremont, CA, USA). All qPCR reactions were conducted in triplicate for each primer set and a non-template negative control was included for each run. Specifically, a threshold cycle (CT) of 31 was used as the detection limit and multiple melting peaks; amplification efficiencies outside the range of 0.9–1.1 were discarded.

Data and statistical analyses

The 16S rRNA gene raw reads were processed by the QIIME2 v2020.08 pipeline (Bolyen et al. 2019). Briefly, paired-end reads were joined by FLASH v1.2.11 (Magoč & Salzberg 2011), then

sequences were demultiplexed by the q2-demux plugin. Afterwards, plugin q2-dada2 was used to conduct quality control, chimeric sequence removal, and sequence clustering. Taxonomic analyses were conducted using the plugins q2-feature-classifier and SILVA v132 database (Quast et al. 2012). The α diversity of the bacterial communities was represented by the Chao1, Shannon, ACE, and Faith's phylogenetic diversity (PD) indices, which were calculated from the amplicon sequence variants (ASVs) table rarefied to 20,349 sequences in QIIME2 for each sample.

A principal coordinate analysis (PCoA) based on Bray–Curtis and Jaccard distances was conducted to visualize the differentiation among samples (Lepš & Šmilauer 2003). A non-parametric multivariate statistical test, Adonis, was implemented to test for significant differences between the variances of bacterial communities with a $P < 0.05$ significance threshold. The similarity of percentages analysis (SIMPER) was applied to identify the most affected genus between different continuous cropping years using the R package, Vegan (Oksanen et al. 2013). Procrustes included in the Vegan R package was used to compare the congruences of the microbiome and metabolism or functional profiles based on the *P*-values and goodness of fit (m^2). The co-occurrence network analysis and visualization were performed using the interactive platform, Gephi (Cherven 2013). Parameters of the network (e.g., number of nodes and edges, average path length, and network diameter) were calculated using the igraph package in R (Csardi & Nepusz 2006). In each network, the size of each node was proportional to the number of connections (i.e., degrees); the thickness of each connection between two nodes (i.e., edges) was proportional to the Spearman's correlation coefficient ($|r| = 0.6–1$).

Sequence accessions

The bacterial 16S rRNA gene sequencing data are publicly available in the NCBI Short Read Archive (SRA) under Bioproject accession No.: PRJNA759342.

Results

Overall measures of diversity

We obtained 503,330 raw sequences and an average of 41,944 sequences per sample. After quality control and sample normalization, a total of 244,188 sequences were filtered and clustered into 6,745 unique ASVs (Edgar 2018). The coverage of samples was > 93% and the rarefaction curve of each sample approached a saturation plateau (Fig. S1), indicating that the current sequencing depth reflected the microbial composition. The Chao1, ACE, and PD indices were all significantly higher in CCY02 and CCY10 compared with CCY05 (all $P<0.05$) (Table 1). The Shannon index did not significantly differ among groups, indicating that the bacterial diversity measured by the species richness with evenness did not significantly change due to continuous cropping practices.

Samples from the same cropping year clustered tightly, while samples from different years clearly separated, based on the PCoA (Fig. S2). The soil microbial compositions under different treatments were further validated by Adonis statistical tests, which revealed significant dissimilarities among different cropping years (Table S1).

Microbial community composition

Overall, Actinobacteria (average ± standard deviation (SD), 28.84 ± 1.50%) and Proteobacteria (26.88 ± 1.50%) were the dominant phyla across all rhizosphere soil samples. The genera with relative abundances > 1% included *Blastococcus* (2.57 ± 0.30%), *Nocardioides* (2.55 ± 0.39%), *Sphingomonas* (2.44 ± 0.28%), *Bacillus* (1.09 ± 0.30%), and *Solirubrobacter* (1.02 ± 0.04%), but these genera did not significantly differ among continuous cropping years. After comparing the relative abundances of each known taxa among the 3 successive monoculture years, we found that 6 phyla, 5 classes, 11 orders, 23 families, and 47 genera exhibited a straight increasing trend over time, while 5 phyla, 8 classes, 14 orders, 19 families, and 32 genera exhibited the opposite trend. A total of 20 taxa exhibited significant continuously strengthened or weakened tolerance to the long-term continuous cropping of Tibetan barley based on the ANOVA results (Fig. 1), but most of these taxa were low in abundance with a mean relative abundance < 1%. For example, Fibrobacteres is an important phylum of cellulose-degrading bacteria (Ransom-Jones et al. 2012); the genus *Devosia* possesses bioremediation potential (Talwar et al. 2020); and the denitrifying bacteria Noviherbaspirillu (Wu et al. 2021) were significantly upregulated over time. The following significantly decreased over time: Firmicutes, which are plant growth-promoting bacilli (Kumar et al. 2012); Bacillales, which have effective biological control and biodegradation potential (Barathi et al. 2020); Nitrosomonadales, which are related to sulfate and iron reduction; and Desulfuromonadales, which are an order capable of iron and sulfate reduction (Wunder et al. 2021).

A SIMPER analysis was used to detect the main genera that drove the compositional shifts of bacterial communities over time. The results showed that 22, 24, and 25 genera were responsible for > 50% cumulative dissimilarity of the microbial community shifts between CCY02 and CCY05, CCY02 and CCY10, and CCY05 and CCY10, respectively (Fig. 2). Fourteen of these overlapping genera were mainly responsible for the differences between each pair of cropping years (Table S2), and the genera *Nocardioides* had the largest dissimilarity contribution.

Core taxa among different cropping years

The consistency of crop type, planting strategies, and research site may lead to a cohort of rhizosphere soil-shared microbial communities from Tibetan barley, while continuous cropping over time could lead to year-unique taxa in the rhizosphere soil. In this study, the taxa that were simultaneously present in all samples were defined as core or shared taxa, and when their mean

relative abundances (at the genus level) were > or < 1%, they were defined as dominant or rare core taxa and subsequently classified at the phylum, class, order, family, and genus levels (Gobet et al. 2010). At the genus level, the core shared microbiome consisted of nearly 50.87% of all taxa (taxonomic richness) and this percentage reached 60% at the phylum level, however, a proportion of unshared taxa seemed to be sample-specific (Fig. 3A). Surprisingly, the total relative abundances of the core taxa at the genus level occupied > 98% of all sequences on average (Fig. 3A), while unshared taxa, or sample-unique taxa, only occupied 1.66 ± 0.31% of all sequences. A total of 164 core taxa were successfully annotated at the genus level and the relative abundances ranged from 0.02 ± 0.01% to 2.57 ± 0.61% (Table S3). The dominant shared genera among samples were Blastococcus, Nocardioides, Sphingomonas, Bacillus, and Solirubrobacter (Fig. 3B).

Bacterial functional genes

QMEC was implemented to determine the abundances of a wide spectrum of functional genes related to C-, N-, P-, and S-cycling (71 genes in total) in a high-throughput manner. A total of 60 genes were successfully detected by QMEC across 12 samples, including 17 genes related to C-degradation, 13 related to C-fixation, 19 related to N-cycling, 6 related to P-cycling, and 5 related to S-cycling (Table S4). Samples from CCY02 and CCY10 displayed a clear clustered pattern based on the principal components analysis (PCA), while samples from CCY05 were scattered (Fig. S3). The abundances of each gene in 12 samples are presented in Fig. S4. Briefly, we found that the genes involved in hemicellulose degradation (abfA and xylA) were most prevalent in C-degradation. The gene involved in the Wood–Ljungdahl pathway (acsA) and the gene involved in ammonization (UreC) were most abundant in C-fixation and N-cycling, respectively. In P-cycling, the genes involved in organic P mineralization (phoD and phnK) were the dominant genes across samples, while the gene related to S reduction (apsA) and the genes (YedZ and SoxY) related to S oxidation were the main genes in S-cycling.

We employed Z-values to compare differences in cycling genes among different cropping years (Table S5). The long-term continuous cropping of Tibetan barley significantly increased the abundances of genes related to C-degradation ($F = 9.25$, $P = 0.01$) and P-cycling ($F = 5.35$, $P = 0.03$) (Fig. S5A and S5B). The abundances of N-cycling genes increased from CCY02 to CCY05 and decreased by CCY10, but no significant differences were detected between groups (Fig. S5C). We also investigated the relationship between the abundances of functional genes and bacterial diversity (Shannon) (Table S6). Results revealed that only N-cycling significantly correlated with bacterial diversity ($r = -0.71$, $P = 0.01$).

Relationships between taxa and functional genes

The Procrustes analysis showed that there were significant correlations between bacterial composition and functional gene profiles after long-term continuous cropping ($P = 0.012$) (Fig. 4A), but not after short-term continuous cropping ($P = 0.111$) (Fig. 4B). A co-occurrence network was constructed to visualize the relationships between the functional cycling genes and bacterial genera (Fig. 5). Only the interactions between the genera and functional genes were kept, of which 173 nodes and 481 edges (196 positive and 285 negative associations) were obtained. The network had good modularity (0.41) and contained 6 modules; each included tightly connected nodes. Module I, which was the largest, contained 65 nodes, including 43 functional genes and 22 genera; most of the C-, N-, P-, and S-cycling genes were tightly connected with a small group of genera. Nine key genera with a degree value > 10 were identified, including *Saccharothrix*, Planomicrobium, Edaphobaculum, Nitrosospira, Angustibacter, Sanguibacter, Brevibacillus, Caulobacter, and Pantoea. Interestingly, Saccharothrix, Edaphobaculum, Sanguibacter, and Pantoea were positively connected with the functional genes, while Planomicrobium, Nitrosospira, Angustibacter, Brevibacillus, and Caulobacter were mainly negatively connected (Table S7).

We also examined the correlations between the cycling genes and 14 top contributors with the dissimilarities among different cropping years. Results revealed that Ohtaekwangia ($r = 0.64$, $P = 0.02$), Pedobacter ($r = 0.63$, $P = 0.03$), and Gaiella ($r = 0.63$, $P = 0.03$) significantly positively correlated with gmGDH, which is related to C degradation (Fig. 6). With regard to C fixation, Devosia significantly positively correlated with cdaR ($r = 0.66$, $P = 0.02$), while Gaiella significantly positively correlated with frdA ($r = 0.58$, $P = 0.04$) and rbcL ($r = 0.68$, $P = 0.01$). For N-cycling, Devosia and Sphingomonas significantly negatively correlated with amoA2 and nxrA ($P < 0.05$), while Saccharibacillus significantly positively correlated with these genes ($P < 0.05$). For P-cycling, Blastococcus significantly negatively correlated with dsrB ($r = -0.58$, $P = 0.04$), while Marmoricola significantly positively correlated with phnK ($r = 0.60$, $P = 0.04$). No significant correlations were detected between the five major categories of functional genes and 14 top genera (Fig. S6).

Soil metabolic profiles

Using LC-MS/MS-based non-targeted metabolomics, a total of 14,380 metabolites in the soils were obtained and 822 metabolites were annotated based on the human metabolome database (HMDB) and Kyoto Encyclopedia of Genes and Genomes (KEGG) database. Based on the metabolic profiles, we implemented a PCA to uncover the different compositions of metabolites in the soil samples from different continuous cropping years. Results revealed that the first two principal components (PC1 and PC2) explained 62.93% of the total variance and samples from different groups obviously differed from each other (Fig. S7). The varying metabolic

compositions among different groups were further confirmed by the hierarchical clustering of the top 100 metabolites (Fig. S8).

VIP values in the PLS-DA model were calculated to examine the changes in the soil metabolites in greater detail. A total of 440 metabolites with VIP > 1.0 and P < 0.05 (ANOVA) were considered significantly affected by the continuous cropping of Tibetan barley. Further linear regression analyses between the acquired metabolites and enhanced continuous cropping years were conducted. A total of 126 metabolites significantly responded to continuous cropping with an increase in 83 metabolites and decrease in 43 metabolites (Table S8). The changes in metabolites mainly occurred in lipids and lipid-like molecules, organic acids and derivatives, and organoheterocyclic compounds. Lipids and lipid-like molecules had the largest number of metabolites affected by continuous cropping. Moreover, nucleosides, nucleotides, and analogues were mainly upregulated over time, while alkaloids and derivatives were mainly downregulated.

Relationships between taxa and metabolites

First, we applied Procrustes tests to depict the correlations between soil metabolic profiles and the bacterial community structure. Significant correlations were detected between specific metabolites and the bacterial community structure in rhizosphere soils during the long- (P = 0.001) and short-term continuous cropping of Tibetan barley (P = 0.027) (Fig. 7). To elucidate which microbial taxa were responsible for the changes in soil microbial metabolism, an interactive network linking the microbes with significant differences between groups (a total of 100 microbial taxa) and differential metabolites (a of total 126 metabolites) was constructed. Only the interactions between metabolites and microbial taxa were kept. The orders Desulfuromonadales (degree 57) and Nitrosomonadales (degree 19), families Archangiaceae (degree 34), Nocardiaceae (degree 23), and Sanguibacteraceae (degree 11), and genera Terrimicrobium (degree 35), Caldinitratiruptor (degree 34), Dehalogenimonas (degree 21), Rubellimicrobium (degree 15), Aquimonas (degree 13), and Sanguibacter (degree 11) co-occurred most frequently with several differential metabolites, including 4-hydroxyvalsartan, methyl-4-pentanoate, pentigetide, and glaucarubolone-15-O-beta-D-glucopyranoside (Fig. 8). Of these metabolites, the frequently co-occurring ones were downregulated over time, except 4-hydroxyvalsartan.

Discussion

Effects of continuous cropping on microbial community structure and diversity

Soil bacterial diversity may significantly decrease, have no change, or fluctuate after long-term continuous cropping. For instance, Yan et al. (2021) reported that soil bacterial diversity significantly decreased (PD and Shannon) after the continuous cropping of Nicotiana tabacum. Chen et al. (2020b) found that the long-term consecutive monocropping of peanuts led to a

general, albeit insignificant, loss in bacterial diversity. Liu et al. (2020) found that the bacterial diversity (PD and number of operational taxonomic units (OTUs)) was significantly higher after the long-term (13 year) continuous monoculture of soybeans, while no significant differences were detected after the short-term monoculture periods (3 and 5 years). Zhao et al. (2020) showed that bacterial richness (ACE) significantly decreased after 5–10 years of continuous cropping and recovered after 30 years, while bacterial diversity (Shannon) significantly increased after continuous cropping (5, 10, and 30 years). In the present study, bacterial diversity (Shannon) did not differ, but bacterial richness (Chao1 and ACE) and PD significantly declined after short-term continuous cropping of Tibetan barley, which is consistent with the findings of Yao et al. (2020), but surprisingly recovered after long-term continuous cropping (Table 1). This phenomenon may be due to the fact that all environmental filters require specific adaptation strategies for survival; stronger selection acting on bacteria often leads to a new cohort of microbiota that adapt to the environment (Fierer et al. 2007; Meola et al. 2014). Even if the microbial composition is sensitive to environmental disturbances, the community may be resilient and stabilize over time (Allison & Martiny 2008).

After 10 years of continuous cropping of Tibetan barley, Actinobacteria and Proteobacteria were the two main dominant phyla that were enriched in many rhizosphere soils after continuous cropping, such as in sugarcane and cotton (Pang et al. 2021; Xi et al. 2019). Actinobacteria, one of the most widely distributed bacterial phyla found in soils, is known for its key eco-physiological role in plant residue decomposition, as its members possess high proportions of CAZymes and collectively maintain a relatively stable presence during plant residue decomposition in terms of taxonomic composition and functional roles (Bao et al. 2021). Another abundant phylum, Proteobacteria, plays a central role in the cycling of several key elements, including N- (Conthe et al. 2018), C- (Chan et al. 2013), and S-cycling (Zhou et al. 2020). In this study, a total of 20 low abundant taxa (< 1%) significantly increased after continuous cropping, during which planting-promoting bacteria or bacteria with bioremediation abilities significantly decreased.

In the current study, we analyzed the top genera that contributed to the dissimilarities among microbial communities from different continuous cropping years. Of these, five were identified as the dominant shared genera across all soil samples, including Blastococcus, Nocardioides, Sphingomonas, Bacillus, and Solirubrobacter (Table S2). These genera have been frequently detected in the rhizosphere soils after the continuous cropping of different crops, including maize (Zhao et al. 2021), cucumber (Li et al. 2021), cotton (Han et al. 2017), and peanuts (Chen et al. 2018). Solirubrobacter and Blastococcus exhibit heavy metal tolerance and advantages in stress resistance, indicating the promising potential for alleviating polluted soil ecosystems (Hou et al. 2021; Wang et al. 2021). A recent study suggested that Sphingomonas possesses multifaceted functions ranging from the remediation of environmental contamination to producing highly

beneficial phytohormones that promote plant growth (Asaf et al. 2020). Bacillus has multiple medical, environmental, and industrial applications (Khurana et al. 2020). Hence, it is proposed that they may play important roles in the successive monoculture of Tibetan barley.

Functional genes and their interactions with microbes

For the first time, QMEC was applied to determine the relative abundances of key element cycling genes after long-term continuous cropping. We found that overall bacterial composition significantly correlated with functional gene profiles (Fig. 4A), indicating that after long-term continuous cropping, alterations in community functions were mainly affected by alterations in bacterial composition. However, after short-term continuous cropping (CCY02 and CCY05), the functional gene profiles and bacterial compositions had poor consistency (Fig. 4B). Thus, we proposed that the functional gene composition was not mainly mediated by changes in microbial composition after short-term continuous cropping. This may be a result of functional redundancy (Rosenfeld 2002), which contributed to bacterial community tolerance and overall community functioning after the short-term continuous monoculture of Tibetan barley. However, significant fluctuations in the taxonomic composition after the long-term continuous monoculture may potentially reduce the stability of the community, which would thereby become more vulnerable to continuous disturbances (Sheng et al. 2015), ultimately affecting bacterial functional compositions.

Genes related to C-degradation and P-cycling increased over time (Table S5). Hemicellulose degradation (abfA and xylA) was most prevalent in C degradation, indicating the potential loss of soil C storage (Chen et al. 2020a). Organic P mineralization (phoD and phnK) increased after continuous cropping, playing an important role in soil P bioavailability. Meyer et al. (2018) indicated that microbes compensated for single nutrient deficiencies by accelerating P- or N-cycling and may have increased SOC turnover in co-limited subsoils with acquirable P reserves. Collectively, these results indicated that, along with the continuous cropping of Tibetan barley, the activity of hemicellulose degradation increased and accelerated C degradation, while microbes may have acquired greater C or N supplies by promoting organic P mineralization. Furthermore, a set of genera were identified that showed tight correlations with most of the functional genes, indicating their functional potential in the cycling of key elements underlying the continuous monocropping of Tibetan barley (Fig. 5). In a previous study, *Nitrosospira* was the primary ammonia-oxidizing bacteria and was mainly responsible for nitrous oxide production (Lourenço et al. 2018). *Pantoea* fixes N or induces N uptake, thereby promoting N availability in plants (Loiret et al. 2004; Singh et al. 2020). Additionally, *Brevibacillus* was reported to have desulfurization activity (Nassar et al. 2013).

A previous study pointed out that the continuous cropping of Tibetan barley significantly increased the bacteria associated with chemo-heterotrophy, aromatic compound degradation, and

nitrate reduction (Yao et al. 2020). This study showed that the dominant shared genera, *Sphingomonas*, exerted significant negative effects on nitrification gene abundances (amoA and nxrA), leading to the imbalance of nitrification and denitrification. Additionally, a previous study showed that *Sphingomonas* in vegetable systems utilized contaminants originating from pesticide residues as a growth and energy source (Busse et al. 2003).

Soil metabolites and their interactions with microbes

Interactions between the roots and rhizosphere community members are primarily achieved via chemical communication (van Dam & Bouwmeester 2016). Shen et al. (2020) observed distinct differences in the metabolite composition over different continuous cropping seasons in tobacco. Our study explored alterations in soil metabolic profiles, which were significantly mediated by soil microbial communities, indicating that certain metabolic pathways were altered and is a primary strategy for soil microbial communities to adapt to environmental stress (Fig. 7). Obvious differences in the patterns of metabolite compositions over time were observed (Figs. S7 and S8), in which the primary metabolites related to lipid and nucleoside metabolism were significantly upregulated, while secondary metabolites, such as alkaloids and derivatives, were significantly downregulated. A previous study pointed out that secondary metabolites greatly affect the microbial community, where some microbes are exploited for their antibiotic and pharmaceutical activities, and others are involved in disease interactions with plants or animals (Fox & Howlett 2008).

We found that the hub taxa Desulfuromonadales mainly co-occurred with metabolites in either negative or positive correlations (Fig. 8), indicating potential important interactions between them. A previous study suggested that positive co-occurrences indicated that the metabolites may be compounds secreted by microbes, while negative co-occurrences may be due to specific microbial consumption or degradation (Devi et al. 2017). Phylogenetically related species within the order Desulfuromonadales utilize different electron exchange pathways (Rotaru et al. 2012). These findings indicated that soil metabolomics can be used to assess the adaptations of soil microbial communities to continuous cropping strategies at the molecular level.

Conclusions

Collectively, we analyzed the changing trends of bacterial composition and diversity after the continuous cropping of Tibetan barley using 16S high-throughput sequencing. After short-term continuous cropping, bacterial richness and PD significantly decreased, but recovered after long-term continuous cropping. We identified five dominant shared genera that were the main contributors to the dissimilarities among bacterial communities from different continuous cropping years, as uncovered by the core taxa and SIMPER analyses. Then, QMEC and

untargeted metabolism were employed to determine the main functional genes and soil metabolites, as well as their changing trends after different continuous cropping years. We further predicted the potential correlations between microbiota and metabolism, including functional genes and soil metabolites. Through this study, we gained further insights into the ecological roles of rhizosphere soil microorganisms underlying the continuous cropping of Tibetan barley.

Acknowledgements

We thank LetPub (www.letpub.com) for its linguistic assistance during the preparation of this manuscript.

References

Alami MM, Xue J, Ma Y, Zhu D, Gong Z, Shu S, and Wang X. 2020. Structure, diversity, and composition of bacterial communities in rhizospheric soil of coptis chinensis franch under continuously cropped fields. *Diversity* 12:57.

Allison SD, and Martiny JB. 2008. Resistance, resilience, and redundancy in microbial communities. *Proceedings of the National Academy of Sciences* 105:11512-11519.

Asaf S, Numan M, Khan AL, and Al-Harrasi A. 2020. Sphingomonas: from diversity and genomics to functional role in environmental remediation and plant growth. *Critical reviews in biotechnology* 40:138-152.

Bao Y, Dolfing J, Guo Z, Chen R, Wu M, Li Z, Lin X, and Feng Y. 2021. Important ecophysiological roles of non-dominant Actinobacteria in plant residue decomposition, especially in less fertile soils. *Microbiome* 9:1-17.

Barathi S, Karthik C, Nadanasabapathi S, and Padikasan IA. 2020. Biodegradation of textile dye Reactive Blue 160 by Bacillus firmus (Bacillaceae: Bacillales) and non-target toxicity screening of their degraded products. *Toxicology reports* 7:16-22.

Bello-Akinosho M, Makofane R, Adeleke R, Thantsha M, Pillay M, and Chirima GJ. 2016. Potential of polycyclic aromatic hydrocarbon-degrading bacterial isolates to contribute to soil fertility. *BioMed Research International* 2016.

Bolyen E, Rideout JR, Dillon MR, Bokulich NA, Abnet CC, Al-Ghalith GA, Alexander H, Alm EJ, Arumugam M, and Asnicar F. 2019. Reproducible, interactive, scalable and extensible microbiome data science using QIIME 2. *Nature biotechnology* 37:852-857.

Busse H-J, Denner EB, Buczolits S, Salkinoja-Salonen M, Bennasar A, and Kämpfer P. 2003. Sphingomonas aurantiaca sp. nov., Sphingomonas aerolata sp. nov. and Sphingomonas faeni sp. nov., air-and dustborne and Antarctic, orange-pigmented, psychrotolerant bacteria, and emended description of the genus Sphingomonas. *International journal of systematic and evolutionary microbiology* 53:1253-1260.

Chan Y, Van Nostrand JD, Zhou J, Pointing SB, and Farrell RL. 2013. Functional ecology of an Antarctic dry valley. *Proceedings of the National Academy of Sciences* 110:8990-8995.

Chen J, Elsgaard L, van Groenigen KJ, Olesen JE, Liang Z, Jiang Y, Lærke PE, Zhang Y, Luo Y, and Hungate BA. 2020a. Soil carbon loss with warming: New evidence from carbon-degrading enzymes. *Global change biology* 26:1944-1952.

520 Chen M, Liu H, Yu S, Wang M, Pan L, Chen N, Wang T, Chi X, and Du B. 2020b. Long-term
521 continuously monocropped peanut significantly changed the abundance and composition
522 of soil bacterial communities. *PeerJ* 8:e9024.
523 Chen W, Teng Y, Li Z, Liu W, Ren W, Luo Y, and Christie P. 2018. Mechanisms by which
524 organic fertilizer and effective microbes mitigate peanut continuous cropping yield
525 constraints in a red soil of south China. *Applied Soil Ecology* 128:23-34.
526 Cherven K. 2013. *Network graph analysis and visualization with Gephi*: Packt Publishing Ltd.
527 Conthe M, Wittorf L, Kuenen JG, Kleerebezem R, van Loosdrecht MC, and Hallin S. 2018. Life
528 on N 2 O: deciphering the ecophysiology of N 2 O respiring bacterial communities in a
529 continuous culture. *The ISME Journal* 12:1142-1153.
530 Csardi G, and Nepusz T. 2006. The igraph software package for complex network research.
531 *InterJournal, complex systems* 1695:1-9.
532 Devi S, Abdul Rehman SA, Tarique KF, and Gourinath S. 2017. Structural characterization and
533 functional analysis of cystathionine β-synthase: an enzyme involved in the reverse
534 transsulfuration pathway of Bacillus anthracis. *The FEBS journal* 284:3862-3880.
535 Edgar RC. 2018. Updating the 97% identity threshold for 16S ribosomal RNA OTUs.
536 *Bioinformatics* 34:2371-2375.
537 Fierer N, Bradford MA, and Jackson RB. 2007. Toward an ecological classification of soil
538 bacteria. *Ecology* 88:1354-1364.
539 Fox EM, and Howlett BJ. 2008. Secondary metabolism: regulation and role in fungal biology.
540 *Current opinion in microbiology* 11:481-487.
541 Gao Z, Han M, Hu Y, Li Z, Liu C, Wang X, Tian Q, Jiao W, Hu J, and Liu L. 2019. Effects of
542 continuous cropping of sweet potato on the fungal community structure in rhizospheric
543 soil. *Frontiers in microbiology* 10:2269.
544 Gobet A, Quince C, and Ramette A. 2010. Multivariate Cutoff Level Analysis (MultiCoLA) of
545 large community data sets. *Nucleic acids research* 38:e155-e155.
546 Han G, Lan J, Chen Q, Yu C, and Bie S. 2017. Response of soil microbial community to
547 application of biochar in cotton soils with different continuous cropping years. *Scientific*
548 *reports* 7:1-11.
549 Hou F, Du J, Yuan Y, Wu X, and Zhao S. 2021. Analysis of Microbial Communities in Aged
550 Refuse Based on 16S Sequencing. *Sustainability* 13:4111.
551 Huang L-F, Song L-X, Xia X-J, Mao W-H, Shi K, Zhou Y-H, and Yu J-Q. 2013. Plant-soil
552 feedbacks and soil sickness: from mechanisms to application in agriculture. *Journal of*
553 *chemical ecology* 39:232-242.
554 Khurana H, Sharma M, Verma H, Lopes BS, Lal R, and Negi RK. 2020. Genomic insights into
555 the phylogeny of Bacillus strains and elucidation of their secondary metabolic potential.
556 *Genomics* 112:3191-3200.
557 Kumar P, Khare S, and Dubey R. 2012. Diversity of bacilli from disease suppressive soil and
558 their role in plant growth promotion and yield enhancement. *New York Sci J* 5:90-111.
559 Kuzyakov Y. 2010. Priming effects: Interactions between living and dead organic matter. *Soil*
560 *Biology and Biochemistry* 42:1363-1371.
561 Lal R. 2016. Soil health and carbon management. *Food and Energy Security* 5:212-222.
562 Lepš J, and Šmilauer P. 2003. *Multivariate analysis of ecological data using CANOCO*:
563 Cambridge university press.

564 Li Y, Chi J, Ao J, Gao X, Liu X, Sun Y, and Zhu W. 2021. Effects of Different Continuous
565 Cropping Years on Bacterial Community and Diversity of Cucumber Rhizosphere Soil in
566 Solar-Greenhouse. *Current Microbiology* 78:2380-2390.
567 Liu Z, Liu J, Yu Z, Yao Q, Li Y, Liang A, Zhang W, Mi G, Jin J, and Liu X. 2020. Long-term
568 continuous cropping of soybean is comparable to crop rotation in mediating microbial
569 abundance, diversity and community composition. *Soil and Tillage Research*
570 197:104503.
571 Loiret F, Ortega E, Kleiner D, Ortega-Rodés P, Rodes R, and Dong Z. 2004. A putative new
572 endophytic nitrogen-fixing bacterium Pantoea sp. from sugarcane. *Journal of applied*
573 *microbiology* 97:504-511.
574 Lourenço KS, Cassman NA, Pijl AS, van Veen JA, Cantarella H, and Kuramae EE. 2018.
575 Nitrosospira sp. govern nitrous oxide emissions in a tropical soil amended with residues
576 of bioenergy crop. *Frontiers in microbiology* 9:674.
577 Magoč T, and Salzberg SL. 2011. FLASH: fast length adjustment of short reads to improve
578 genome assemblies. *Bioinformatics* 27:2957-2963.
579 Meola M, Lazzaro A, and Zeyer J. 2014. Diversity, resistance and resilience of the bacterial
580 communities at two alpine glacier forefields after a reciprocal soil transplantation.
581 *Environmental microbiology* 16:1918-1934.
582 Meyer N, Welp G, Rodionov A, Borchard N, Martius C, and Amelung W. 2018. Nitrogen and
583 phosphorus supply controls soil organic carbon mineralization in tropical topsoil and
584 subsoil. *Soil Biology and Biochemistry* 119:152-161.
585 Murphy CE, and Lemerle D. 2006. Continuous cropping systems and weed selection. *Euphytica*
586 148:61-73.
587 Nassar HN, El-Gendy NS, Mostafa Y, Mahdy H, and El-Temtamy S. 2013. Desulfurization of
588 dibenzothiophene by a novel strain Brevibacillus invocatus C19 isolated from Egyptian
589 coke. *Biosciences Biotechnology Research Asia* 10.
590 Oksanen J, Blanchet FG, Kindt R, Legendre P, Minchin PR, O'hara R, Simpson GL, Solymos P,
591 Stevens MHH, and Wagner H. 2013. Package 'vegan'. *Community ecology package,*
592 *version* 2:1-295.
593 Pang Z, Dong F, Liu Q, Lin W, Hu C, and Yuan Z. 2021. Soil metagenomics reveals effects of
594 continuous sugarcane cropping on the structure and functional pathway of rhizospheric
595 microbial community. *Frontiers in microbiology* 12:369.
596 Pervaiz ZH, Iqbal J, Zhang Q, Chen D, Wei H, and Saleem M. 2020. Continuous cropping alters
597 multiple biotic and abiotic indicators of soil health. *Soil Systems* 4:59.
598 Pii Y, Borruso L, Brusetti L, Crecchio C, Cesco S, and Mimmo T. 2016. The interaction between
599 iron nutrition, plant species and soil type shapes the rhizosphere microbiome. *Plant*
600 *Physiology and Biochemistry* 99:39-48.
601 Pinton R, Varanini Z, and Nannipieri P. 2007. *The rhizosphere: biochemistry and organic*
602 *substances at the soil-plant interface*: CRC press.
603 Quast C, Pruesse E, Yilmaz P, Gerken J, Schweer T, Yarza P, Peplies J, and Glöckner FO. 2012.
604 The SILVA ribosomal RNA gene database project: improved data processing and web-
605 based tools. *Nucleic acids research* 41:D590-D596.
606 Ransom-Jones E, Jones DL, McCarthy AJ, and McDonald JE. 2012. The Fibrobacteres: an
607 important phylum of cellulose-degrading bacteria. *Microbial ecology* 63:267-281.

Rinot O, Levy GJ, Steinberger Y, Svoray T, and Eshel G. 2019. Soil health assessment: A critical review of current methodologies and a proposed new approach. *Science of the Total Environment* 648:1484-1491.

Rosenfeld JS. 2002. Functional redundancy in ecology and conservation. *Oikos* 98:156-162.

Rotaru A-E, Shrestha PM, Liu F, Ueki T, Nevin K, Summers ZM, and Lovley DR. 2012. Interspecies electron transfer via hydrogen and formate rather than direct electrical connections in cocultures of Pelobacter carbinolicus and Geobacter sulfurreducens. *Applied and environmental microbiology* 78:7645-7651.

Schad P, and Spaargaren O. 2006. *World reference base for soil resources 2006: A framework for international classification, correlation and communication*: Food and agriculture organization of the United nations (FAO).

Shen H, Yan W, Yang X, He X, Wang X, Zhang Y, Wang B, and Xia Q. 2020. Co-occurrence network analyses of rhizosphere soil microbial PLFAs and metabolites over continuous cropping seasons in tobacco. *Plant and Soil* 452:119-135.

Sheng Z, Van Nostrand JD, Zhou J, and Liu Y. 2015. The effects of silver nanoparticles on intact wastewater biofilms. *Frontiers in microbiology* 6:680.

Singh P, Singh RK, Li H-B, Guo D-J, Sharma A, Lakshmanan P, Malviya MK, Song X-P, Solanki MK, and Verma KK. 2020. Diazotrophic bacteria Pantoea dispersa and Enterobacter asburiae promote sugarcane growth by inducing nitrogen uptake and defense-related gene expression. *Frontiers in microbiology* 11.

Sun J, Zou L, Li W, Wang Y, Xia Q, and Peng M. 2018. Soil microbial and chemical properties influenced by continuous cropping of banana. *Scientia Agricola* 75:420-425.

Swenson TL, Jenkins S, Bowen BP, and Northen TR. 2015. Untargeted soil metabolomics methods for analysis of extractable organic matter. *Soil Biology and Biochemistry* 80:189-198.

Talwar C, Nagar S, Kumar R, Scaria J, Lal R, and Negi RK. 2020. Defining the environmental adaptations of genus Devosia: Insights into its expansive short peptide transport system and positively selected genes. *Scientific reports* 10:1-18.

van Dam NM, and Bouwmeester HJ. 2016. Metabolomics in the rhizosphere: tapping into belowground chemical communication. *Trends in plant science* 21:256-265.

Wang Q, Li Z, Li X, Ping Q, Yuan X, Agathokleous E, and Feng Z. 2021. Interactive effects of ozone exposure and nitrogen addition on the rhizosphere bacterial community of poplar saplings. *Science of the Total Environment* 754:142134.

Wang Y, Zhu S, Liu T, Guo B, Li F, and Bai X. 2020. Identification of the rhizospheric microbe and metabolites that led by the continuous cropping of ramie (Boehmeria nivea L. Gaud). *Scientific reports* 10:1-11.

Withers E, Hill PW, Chadwick DR, and Jones DL. 2020. Use of untargeted metabolomics for assessing soil quality and microbial function. *Soil Biology and Biochemistry* 143:107758.

Wu Y-F, Chai C-W, Li Y-N, Chen J, Yuan Y, Hu G, Rosen BP, and Zhang J. 2021. Anaerobic As (III) oxidation coupled with nitrate reduction and attenuation of dissolved Arsenic by Noviherbaspirillum Species. *ACS Earth and Space Chemistry* 5:2115-2123.

Wunder LC, Aromokeye DA, Yin X, Richter-Heitmann T, Willis-Poratti G, Schnakenberg A, Otersen C, Dohrmann I, Römer M, and Bohrmann G. 2021. Iron and sulfate reduction structure microbial communities in (sub-) Antarctic sediments. *The ISME Journal*:1-18.

Xi H, Shen J, Qu Z, Yang D, Liu S, Nie X, and Zhu L. 2019. Effects of long-term cotton continuous cropping on soil microbiome. *Scientific reports* 9:1-11.

Yan L, Zhang W, Duan W, Zhang Y, Zheng W, and Lai X. 2021. Temporal Bacterial Community Diversity in the Nicotiana tabacum Rhizosphere Over Years of Continuous Monocropping. *Frontiers in microbiology* 12:1276.

Yang C, Liu N, and Zhang Y. 2019. Soil aggregates regulate the impact of soil bacterial and fungal communities on soil respiration. *Geoderma* 337:444-452.

Yao Y, Yao X, An L, Bai Y, Xie D, and Wu K. 2020. Rhizosphere Bacterial Community Response to Continuous Cropping of Tibetan Barley. *Frontiers in microbiology* 11:551444-551444.

Yu L, Tang Y, Wang Z, Gou Y, and Wang J. 2019. Nitrogen-cycling genes and rhizosphere microbial community with reduced nitrogen application in maize/soybean strip intercropping. *Nutrient Cycling in Agroecosystems* 113:35-49.

Zeng Q, and An S. 2021. Identifying the Biogeographic Patterns of Rare and Abundant Bacterial Communities Using Different Primer Sets on the Loess Plateau. *Microorganisms* 9:139.

Zhang Y, Li P, Liu X, Xiao L, Shi P, and Zhao B. 2019. Effects of farmland conversion on the stoichiometry of carbon, nitrogen, and phosphorus in soil aggregates on the Loess Plateau of China. *Geoderma* 351:188-196.

Zhao J, Zhang D, Yang Y, Pan Y, Zhao D, Zhu J, Zhang L, and Yang Z. 2020. Dissecting the effect of continuous cropping of potato on soil bacterial communities as revealed by high-throughput sequencing. *PloS one* 15:e0233356.

Zhao Y, Fu W, Hu C, Chen G, Xiao Z, Chen Y, Wang Z, and Cheng H. 2021. Variation of rhizosphere microbial community in continuous mono-maize seed production. *Scientific reports* 11:1-13.

Zheng B, Zhu Y, Sardans J, Peñuelas J, and Su J. 2018. QMEC: a tool for high-throughput quantitative assessment of microbial functional potential in C, N, P, and S biogeochemical cycling. *Science China Life Sciences* 61:1451-1462.

Zhou Z, Tran PQ, Kieft K, and Anantharaman K. 2020. Genome diversification in globally distributed novel marine Proteobacteria is linked to environmental adaptation. *The ISME Journal* 14:2060-2077.

Figure 1

Total 20 taxa showed significant feedback continuously strengthening or weakening to the long-term monocropping of Tibetan barley. (A) 10 taxa were increased, while (B) 10 taxa were decreased.

The correlation between the relative abundance of each taxon and enhanced cropping yeas was further validated by ANOVA. $P < 0.05$ was considered significant.

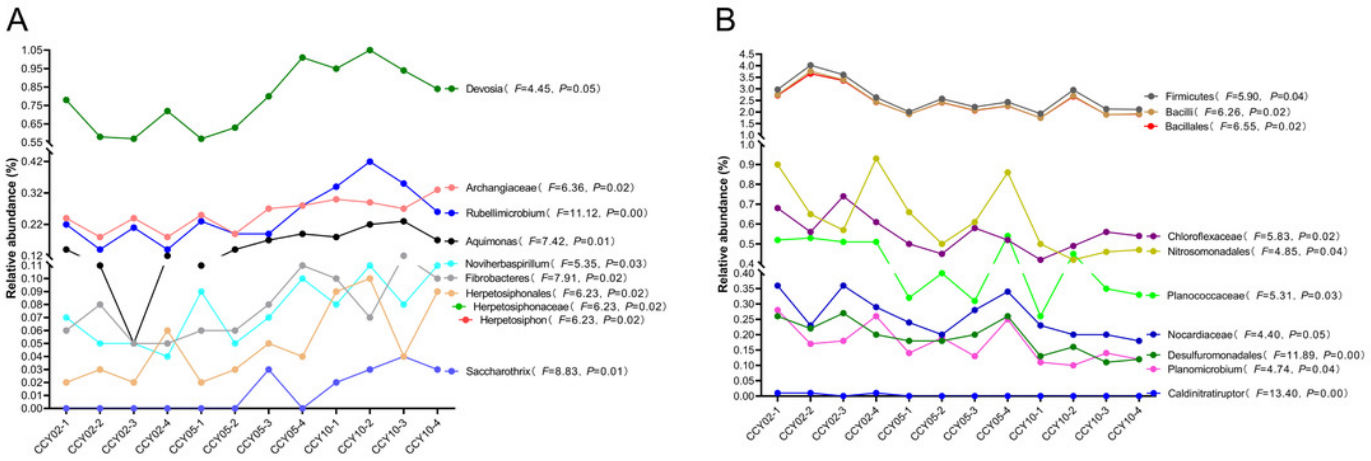

Figure 2

The relative contribution of main genera to the dissimilarity between communities of (A) CCY02 and CCY05, (B) CCY02 and CCY10, and (C) CCY05 and CCY10 by SIMPER analysis.

The main genera was listed when cumulative dissimilarity over 50% in each group.

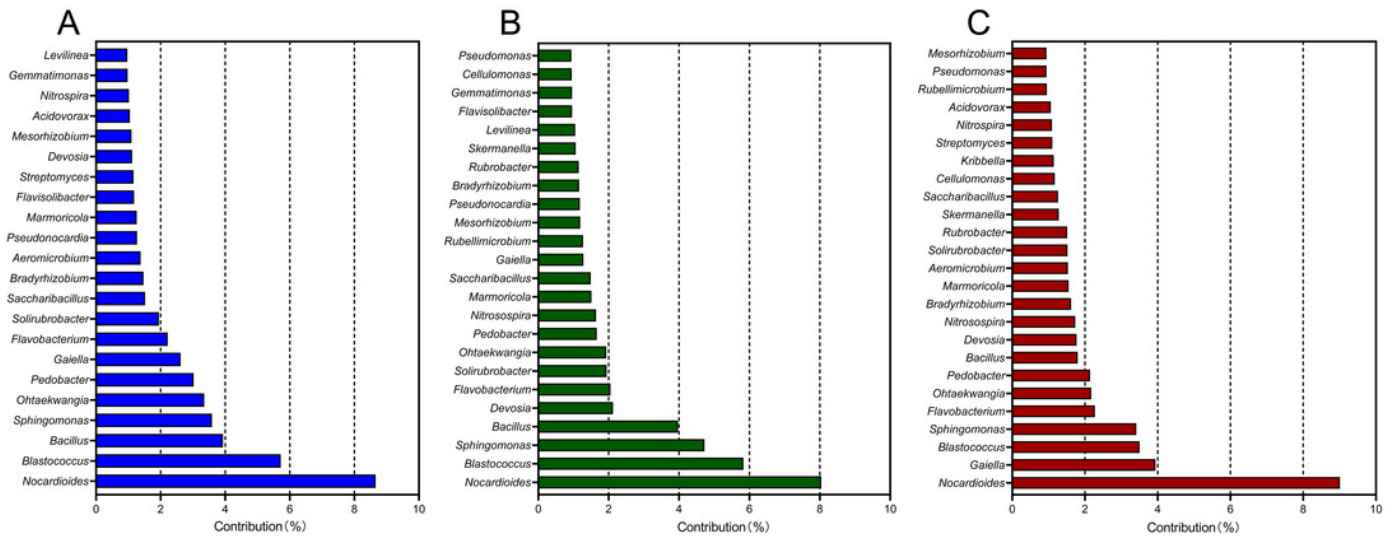

Figure 3

Richness, abundance, and identity of taxa are shared across all rhizosphere soil samples. (A) Richness and sequence coverage of shared taxa in all the samples. (B) Heatmap of the top 20 shared genera among samples.

Relative abundances were log-transformed and colored from blue to red to indicate high-to-low relative abundances. Shared genera were identified as dominant (>1% relative abundance) or rare (<1% relative abundance) in each group. The name of each genus is colored by phylum class.

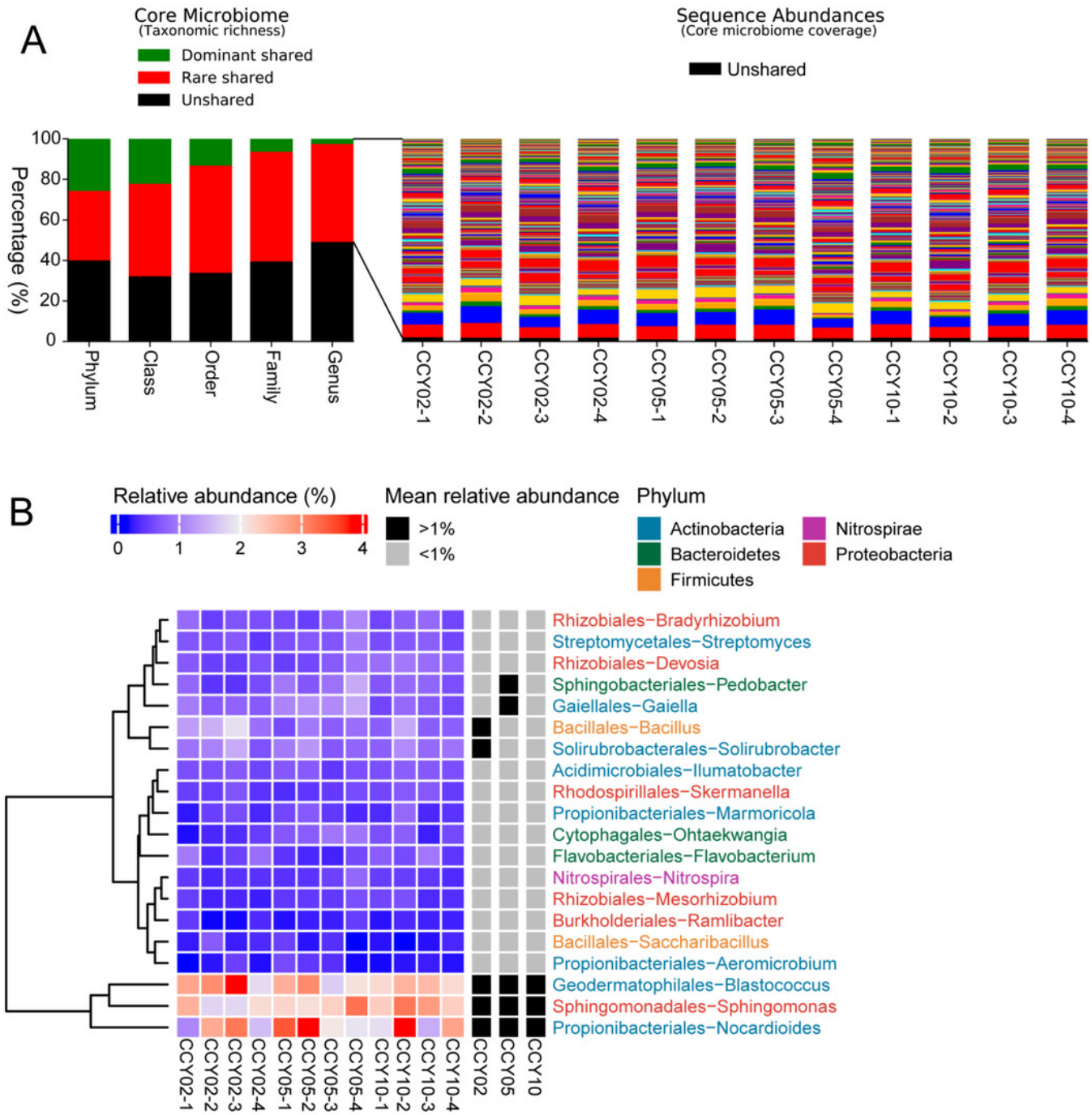
A
Core Microbiome
(Taxonomic richness)
Dominant shared
Rare shared
Unshared
Sequence Abundances
(Core microbiome coverage)
Unshared
Percentage (%)
100
80
60
40
20
0
Phylum
Class
Order
Family
Genus
CCY02-1
CCY02-2
CCY02-3
CCY02-4
CCY05-1
CCY05-2
CCY05-3
CCY05-4
CCY10-1
CCY10-2
CCY10-3
CCY10-4
B
Relative abundance (%)
0
1
2
3
4
Mean relative abundance
>1%
<1%
Phylum
Actinobacteria
Bacteroidetes
Firmicutes
Nitrospirae
Proteobacteria
Rhizobiales−Bradyrhizobium
Streptomycetales−Streptomyces
Rhizobiales−Devosia
Sphingobacteriales−Pedobacter
Gaiellales−Gaiella
Bacillales−Bacillus
Solirubrobacterales−Solirubrobacter
Acidimicrobiales−Ilumatobacter
Rhodospirillales−Skermanella
Propionibacteriales−Marmoricola
Cytophagales−Ohtaekwangia
Flavobacteriales−Flavobacterium
Nitrospirales−Nitrospira
Rhizobiales−Mesorhizobium
Burkholderiales−Ramlibacter
Bacillales−Saccharibacillus
Propionibacteriales−Aeromicrobium
Geodermatophilales−Blastococcus
Sphingomonadales−Sphingomonas
Propionibacteriales−Nocardioides
CCY02-1
CCY02-2
CCY02-3
CCY02-4
CCY05-1
CCY05-2
CCY05-3
CCY05-4
CCY10-1
CCY10-2
CCY10-3
CCY10-4
CCY02
CCY05
CCY10

Figure 4

Relationships between bacterial community structure and functional gene profiles from QMEC analysis during (A) long-term and (B) short-term of continuous monocropping years, respectively.

The correlation was determined by Procrustes test and considered significanlt when $P < 0.05$.

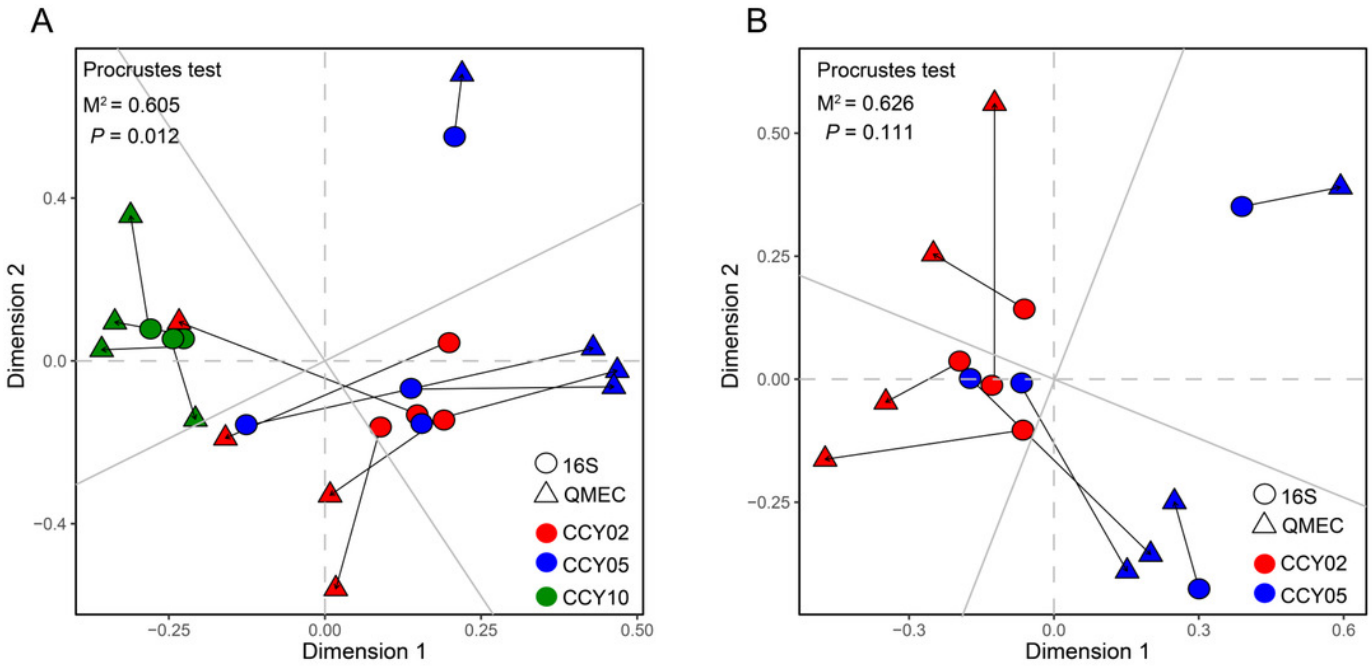

Figure 5

The Co-occurrence network between the functional genes and all the bacterial genera appeared in all rhizosphere soil samples.

A connection indicates a strong ($|r|$ of > 0.6) and significant (P of < 0.05) Spearman's correlation, while only a connection between genera and functional gene was kept. Red lines indicate negative correlations, while green lines indicate positive correlations. The network is colored by module, which clusters the tightly connected nodes. The size of each node is proportional to the number of connections: The thickness of each edge is proportional to the value of the Spearman correlation. The same node colors represent nodes belonging to the same modules. The font color blue represents the functional gene, while the font-weight represents the genera that clustered tightly within Module I with node degrees larger than 10.

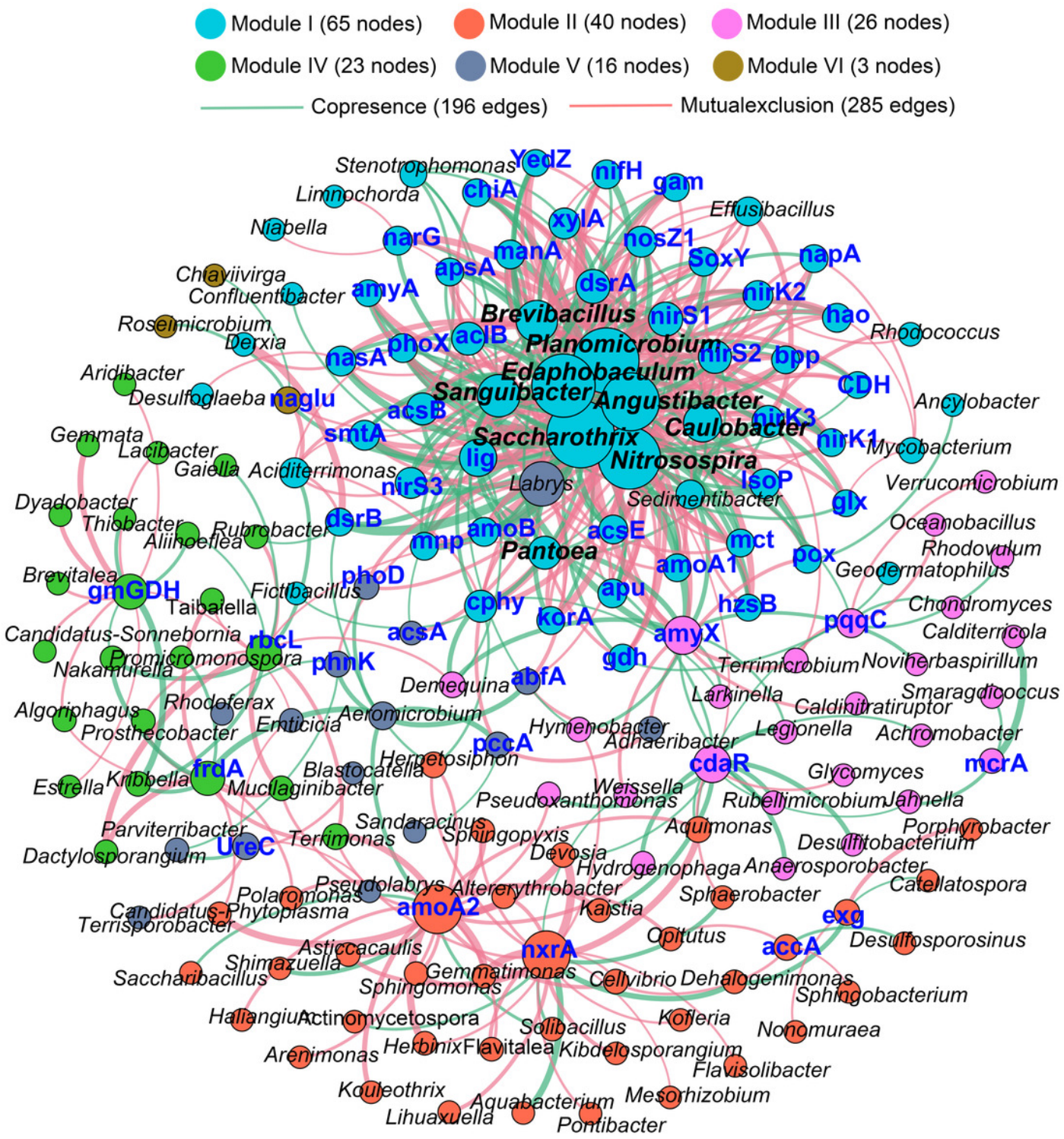
Module I (65 nodes)
Module II (40 nodes)
Module III (26 nodes)
Module IV (23 nodes)
Module V (16 nodes)
Module VI (3 nodes)
Copresence (196 edges)
Mutualexclusion (285 edges)
YedZ
nifH
gam
chiA
xylA
narG
nosZ1
SoxY
napA
manA
apsA
dsrA
amyA
nirK2
nirS1
hao
phoX
aclB
nasA
nirS2
bpp
CDH
naglu
acsB
smtA
nirK3
nirK1
lig
isoP
nirS3
glx
dsrB
amoB
acsE
mct
pox
mnp
amoA1
phoD
apu
gmGDH
cphy
hzsB
pqqC
korA
acsA
amyX
rbcL
phnK
gdh
abfA
pccA
cdaR
mcrA
frdA
UreC
amoA2
nxrA
exg
accA
Brevibacillus
Planomicrobium
Edaphobaculum
Sanguibacter
Angustibacter
Saccharothrix
Caulobacter
Nitrosospira
Pantoea
Stenotrophomonas
Limnochorda
Effusibacillus
Niabella
Chryseobacterium
Confluentibacter
Roseimicrobium
Derxia
Rhodococcus
Aridibacter
Desulfoglaeba
Ancylobacter
Gemmata
Lacibacter
Gaiella
Aciditerrimonas
Mycobacterium
Labrys
Verrucomicrobium
Sedimentibacter
Dyadobacter
Thiobacter
Rubrobacter
Oceanobacillus
Aliihoeflea
Rhodovulum
Brevitalea
Fictibacillus
Geodermatophilus
Taibaiella
Chondromyces
Candidatus-Sonnebornia
Calditerricola
Promicromonospora
Nakamurella
Terrimicrobium
Novoherbaspirillum
Demequina
Larkinella
Smaragdicoccus
Algoriphagus
Rhodoferax
Caldinitratiruptor
Prosthecobacter
Ernticicia
Aeromicrobium
Hymenobacter
Adhaeribacter
Legionella
Achromobacter
Hergetosiphon
Glycomyces
Estrella
Kribbella
Blastocatella
Mucilaginibacter
Weissella
Pseudoxanthomonas
Rubellimicrobium
Jahnella
Parviterribacter
Sandaracinus
Terrimonas
Sphingopyxis
Aquimonas
Porphyrobacter
Dactylosporangium
Devosia
Desulfitobacterium
Hydrogenophaga
Anaerosporobacter
Pseudolabrys
Altererythrobacter
Sphaerobacter
Catellatospora
Polaromonas
Candidatus-Phytoplasma
Kaistia
Terrisporobacter
Opitutus
Desulfosporosinus
Asticcacaulis
Shimazuella
Gemmatimonas
Cellvibrio
Dehalogenimonas
Saccharibacillus
Sphingomonas
Sphingobacterium
Haliangium
Actinomycetospora
Solibacillus
Koleria
Nonomuraea
Herbinix
Flavitalea
Kibdelosporangium
Arenimonas
Flavisolibacter
Kouleothrix
Aquabacterium
Mesorhizobium
Lihuaxuella
Pontibacter

Figure 6

Correlations between the main overlapped genera (detected by SIMPER analysis) with the functional genes in rhizosphere soils.

Heatmap values ranged from +0.5 to -0.5. Values above/below zero represent positive/negative correlations. *$P < 0.05$ was considered significant, while **$P < 0.01$ was considered extremely significant.

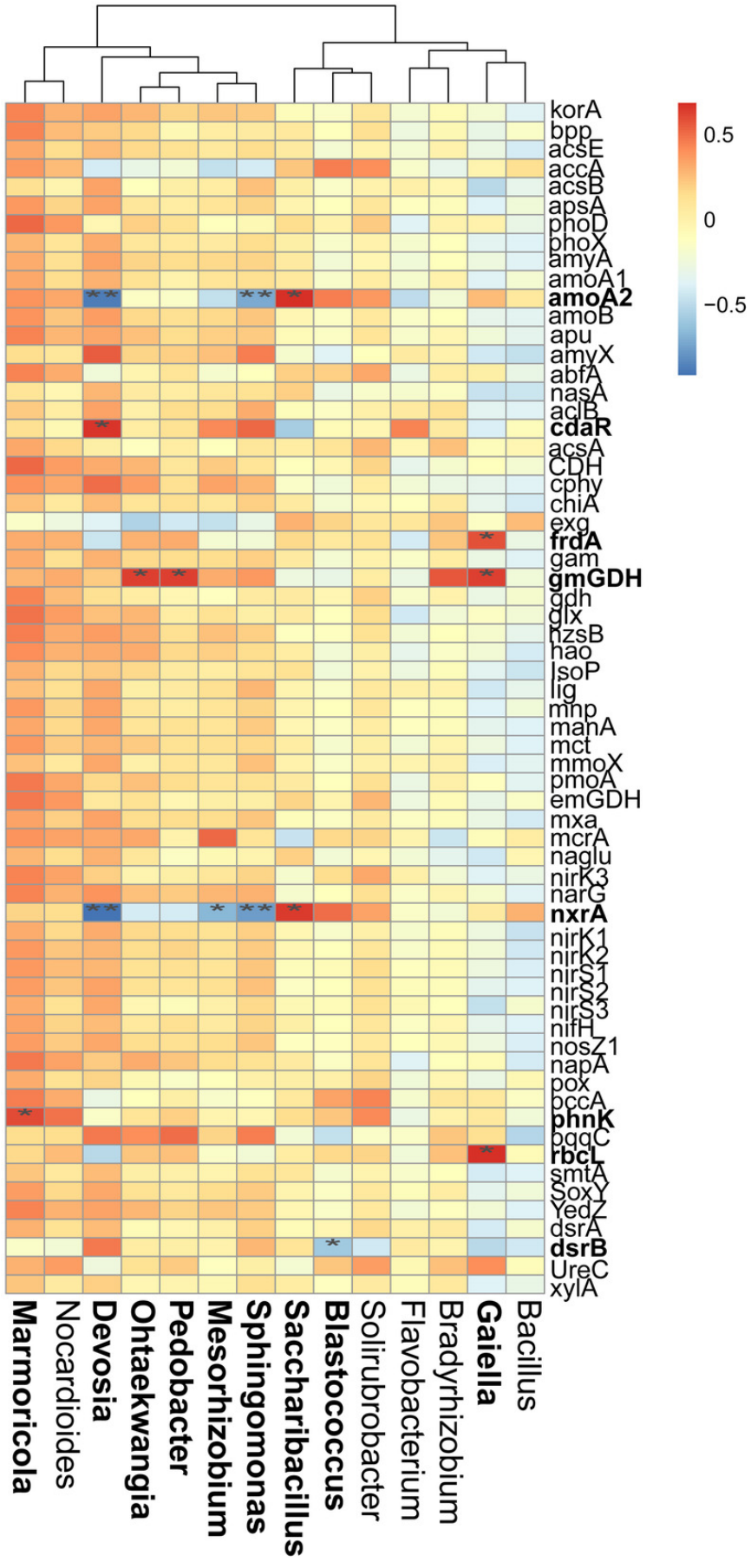
0.5
0
−0.5
korA
bpp
acsE
accA
acsB
apsA
phoD
phoX
amyA
amoA1
amoA2
amoB
apu
amyX
abfA
nasA
aclB
cdaR
acsA
CDH
cphy
chiA
exg
frdA
gam
gmGDH
gdh
glx
hzsB
hao
IsoP
lig
mnp
manA
mct
mmoX
pmoA
emGDH
mxa
mcrA
naglu
nirK3
narG
nxrA
nirK1
nirK2
nirS1
nirS2
nirS3
nifH
nosZ1
napA
pox
pccA
phnK
pqqC
rbcL
smtA
SoxY
YedZ
dsrA
dsrB
UreC
xylA
Marmoricola
Nocardioides
Devosia
Ohtaekwangia
Pedobacter
Mesorhizobium
Sphingomonas
Saccharibacillus
Blastococcus
Solirubrobacter
Flavobacterium
Bradyrhizobium
Gaiella
Bacillus

Figure 7

Relationships between bacterial community structure and Functional gene profiles from non-targeted metabolomic analysis during (A) long-term and (B) short-term of continuous monocropping years, respectively.

The correlation was determined by Procrustes test and considered significanlt when $P < 0.05$.

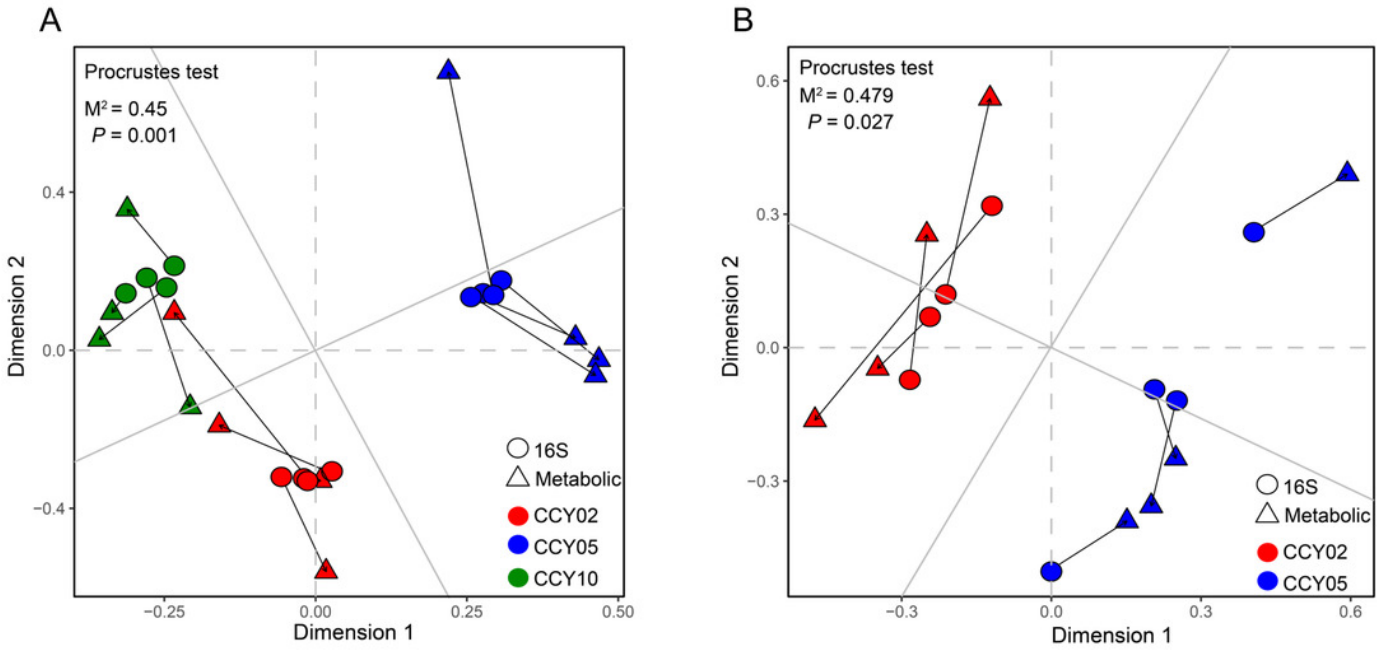

Figure 8

The network between the differential expressed metabolites and differentially abundant genera among different cropping years.

A connection indicates a very strong (|*r*| of > 0.9) and significant (*P* of < 0.01) Spearman's correlation, while only a connection between genera and functional gene was kept. Red lines indicate negative correlations, while green lines indicate positive correlations. The size of each node is proportional to the number of connections: The thickness of each edge is proportional to the value of the Spearman correlation.

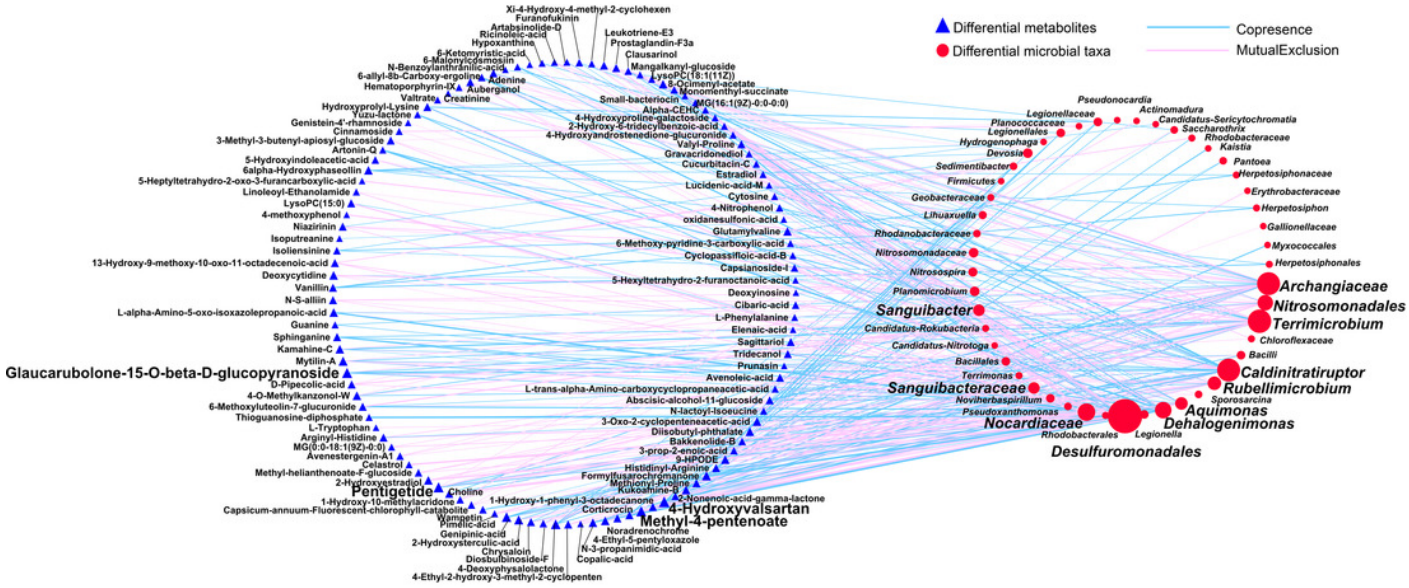

Table 1(on next page)

The significant difference of alpha index among groups by the ANOVA test.

Values represent means ± standard deviation (n = 4). Different lowercase letters within the same column indicate significant differences among different continuous cropping durations at $P < 0.05$ according to Duncan's test.

Table 1. The significant difference of alpha index among groups by the ANOVA test.

	Chao1	ACE	PD	Shannon
CCY02	4746.71±155.81a	4825.48±137.84a	179.89±7.65a	9.69±0.16a
CCY05	4344.43±195.09b	4387.67±188.26b	162.66±4.50b	9.51±0.09a
CCY10	4769.57±164.57a	4886.41±137.82a	178.89±3.22a	9.72±0.06a

Values represent means ± standard deviation (n = 4). Different lowercase letters within the same column indicate significant differences among different continuous cropping durations at $P < 0.05$ according to Duncan's test.